Journal of Alloys and Compounds 660 (2016) 148–158

Contents lists available at ScienceDirect

Journal of Alloys and Compounds

journal homepage: http://www.elsevier.com/locate/jalcom

A method to determine contributions to the hyperfine field at Ce probes in magnetic hosts: Application to Ce impurities at RE sites in REAg (RE = Gd, Tb, Dy, Ho) compounds

F.H.M. Cavalcante, L.F.D. Pereira, A.W. Carbonari*, J. Mestnik-Filho, R.N. Saxena

Instituto de Pesquisas Energéticas e Nucleares – IPEN/CNEN-SP, Universidade de São Paulo, Av. Prof. Lineu Prestes, 2242, 05508-000, São Paulo, SP, Brazil

ARTICLE INFO

Article history:
Received 8 September 2015
Accepted 12 November 2015
Available online 1 December 2015

Keywords:
Magnetic hyperfine field
Localized moments
Exchange interaction

ABSTRACT

In this paper, a model based on the molecular field theory is used to fit experimental data of the magnetic hyperfine field (mhf) at nuclei of a magnetic dilute impurity in a magnetic host and determine separately the contributions of the host and the impurity to mhf, which otherwise would not be possible. The model is used to fit data on the temperature dependence of mhf at ^{140}Ce nuclei as an impurity replacing rare-earth (RE) ions in REAg (RE = Gd, Tb, Dy, Ho) hosts. Experimental data on GdAg and DyAg are available in the literature and data on the temperature dependence of mhf for TbAg and HoAg were measured by perturbed gamma–gamma angular correlation (PAC) spectroscopy. Due to the magnetic interplay between host and impurity magnetic ions, the behavior of the temperature dependence of mhf below respective T_N of each compound shows an accentuated deviation from an expected Brillouin-like pattern for each compound. This unusual behavior is a consequence of an additional magnetic interaction which emerges from the polarization of localized moments of Ce induced by the magnetic field from RE ions. The impurity contribution calculated from the model are shown to follow the same behavior of the reduced hyperfine field determined from experimental data. The host contribution is discussed in terms of the indirect magnetic coupling between the magnetic RE ions of the host and the obtained values are supported by first-principles calculations based on the density functional theory (DFT). It is also shown that both contributions calculated by the model have values within the expected experimental systematic. Moreover, density of states (DOS) from first-principles calculations explain the mechanism responsible by the observed anomalous behavior of the temperature dependence of mhf. The model presented here can be applied to understand the complex phenomenon of interactions between the magnetic ions of a ordered host and dilute magnetic impurity atoms. The physical description of these magnetic interactions might have an important impact to new applications in spintronics and quantum computing.

1. Introduction

The investigation of magnetism from an atomic view in intermetallic compounds containing rare-earth elements is useful to understand the wide variety of interesting physical phenomena, especially different magnetic behaviors, associated with these materials. Neutron diffraction is one of the techniques often used to obtain information about the spatial distribution of the magnetic moments in magnetic compounds. Unfortunately, due to the very large thermal neutron absorption cross sections of some rare-earth elements, little information is available from neutron diffraction studies about details of the magnetic structure in many rare-earth compounds. Nevertheless, as experimental data on the local magnetism at a certain site in magnetic compounds is very important to study the origin of its magnetic properties, other techniques can be used. Hyperfine interaction (hfi) techniques are very useful tools to provide precise and reliable information on the magnetism in an atomic scale. Hfi techniques measure the local magnetic field at a certain site of the samples by using probe nuclei. Some hfi techniques based on resonance methodology use the constituent rare-earth element nucleus itself as a probe, this is the case, for instance, of ^{151}Eu, ^{155}Gd, ^{161}Dy and ^{171}Yb in Mössbauer spectroscopy or nuclear magnetic resonance. However, as rare-

* Corresponding author.
E-mail address: carbonar@ipen.br (A.W. Carbonari).

http://dx.doi.org/10.1016/j.jallcom.2015.11.081
0925-8388/

earth ions have incomplete 4*f* shell, contributions to the magnetic hyperfine field (mhf) from the orbital angular momentum or core polarization of the probe atom itself are usually rather large and may be different for each rare-earth ion. As a consequence, in a systematic investigation where a series of compounds with different rare-earth elements are being studied and the magnetic interaction between magnetic rare-earth atoms is the subject of interest, it is not convenient to use hfi probe nuclei that contribute themselves to mhf, because their large 4*f* contribution would mask contributions from the neighborhood. The use of different probes with different magnetic coupling constants is also a problem in such investigations. In a systematic study, therefore, it is better to use the same probe nucleus (in which contributions to mhf from the nucleus itself are not present or can be separated from the host contribution) for all compounds in order to better compare the results. At this point, it is noteworthy that localized moments on diluted magnetic ions in magnetic matrices can only be measured by local techniques such as hfi techniques.

Perturbed gamma–gamma angular correlation (PAC) spectroscopy is a hyperfine interaction technique where radioactive probe nuclei, which emit gamma rays in cascade, are introduced into the samples and the time dependence of the gamma-rays emission pattern are measured. In PAC spectroscopy it is, therefore, possible to use the same probe nucleus to investigate a series of compounds with different rare-earth elements. The most convenient PAC probe nucleus used to investigate the contribution from the magnetic neighbor to the hyperfine field is the closed-shell ^{111}Cd, which can, in principle, substitute for any of the constituent elements in the compound under investigation. However, sometimes this probe does not substitute the rare-earth elements, and some other probe must be used to investigate the local magnetic field at the rare-earth sites.

^{140}Ce is another PAC probe that can be used to investigate the local magnetism in rare-earth compounds as it substitutes rare-earth ions. However, Ce^{+3} ions have one 4*f* electron and consequently a localized moment is found in such ions, which also create a contribution from the probe itself to the magnetic hyperfine field. On the other hand, the 4*f* band of Ce^{+3} is generally located close to the Fermi level in most compounds, especially when Ce is an impurity in a rare-earth compound, and can be hybridized with *d*-band of the host [1]. As a consequence, the influence on the magnetic hyperfine field can be strongly dependent on the temperature and easy to be observed as reported before for measurements of the temperature dependence of the mhf at ^{140}Ce in Gd by Thiel et al. [2] and $CeMn_2Ge_2$ by Carbonari et al. [3], in which the behavior of mhf strongly departs from the standard Brillouin curve.

For closed-shell probe nuclei as impurity in rare earth intermetallic compounds, the magnetic hyperfine field is proportional to the conduction electron spin polarization (CEP) at the probe site, as shown in literature for several compounds using, for instance, ^{111}Cd [4–7]. In the case of rare earth probe nuclei, the 4*f* electrons are expected to contribute significantly to the magnetic hyperfine field. The magnetic hyperfine field measured by PAC spectroscopy is the effective field at the probe site and, therefore, it is not possible to determine each contribution to mhf separately from the measurements. Unfortunately, there are only few experimental results available for rare-earth probe nuclei in rare earth magnetic compounds to permit a systematic investigation of the mhf contribution due to 4*f* electrons. Moreover, it is not known yet the intensity of the contribution of 4*f* electrons of a rare-earth impurity probe on the magnetic hyperfine field in magnetic compounds neither if it is always present.

The magnetic hyperfine field (mhf) at probe nuclei of dilute magnetic rare-earth ions in magnetic intermetallic compounds is itself a very interesting and yet not well understood subject mainly because of the exchange interaction between the localized magnetic moment on the probe atom and the magnetic host ions. The understanding of this interaction is technologically important since the possibility to design a specific material, in which this interaction can be tuned, would make it a potential candidate to new application in spintronics and quantum computing.

In the present paper we show that, using a simple model based on the molecular field theory, it is possible to separately determine both contributions to the effective mhf measured experimentally: one from the magnetic ions of the host and another from the 4*f* electron of the impurity probe atom. As a consequence, such methodology makes ^{140}Ce a useful probe to be used in measurements of local magnetic fields in rare-earth compounds as well as it allows the individual investigation of each contribution, which opens the possibility to study the complex interaction between the host magnetic ions and the Ce magnetic impurity.

In order to verify the applicability of the model it is convenient to test it in magnetic matrices belonging to a series of isostructural RE compounds because parameters such as atomic distances, chemical composition, magnetic ion, etc. can be controlled. We have chosen to investigate in this work the mhf at ^{140}Ce probe nuclei substituting rare-earth (RE) sites of the cubic intermetallic binary compounds of the type REAg in order to quantify the 4*f* contribution and compare the results with previous measurements of mhf on ^{140}Ce in other rare earth compounds. The antiferromagnetic order of the majority of compounds in the family, for instance in NdAg compound [8], is characterized by adjacent ferromagnetic planes (110) having oppositely directed spins in the [001] direction [9–11]. The exceptions are CeAg and PrAg, which orders ferromagnetically [12]. The antiferromagnetic $(\pi,\pi,0)$ structure in these compounds is built up by ferromagnetic [110] planes coupled antiferromagnetically. Considering the lanthanide series from La to Lu, NdAg is the first antiferromagnetic compound after CeAg and PrAg. The antiferromagnetic state in NdAg was shown to be unstable having an energy extremely close to the ferromagnetic state [13]. Phenomena like quadrupole interactions and crystal field splitting, spin fluctuations and incommensurate magnetism make the magnetic behavior in REAg compounds very complex.

In the present work the temperature dependence of mhf at ^{140}Ce on rare-earth sites in TbAg and HoAg was measured by PAC spectroscopy below respective Néel temperatures. The results were analyzed together with previous ones also from PAC measurements using ^{140}Ce at rare-earth sites in GdAg [14] and DyAg [15]. Measurements of mhf at some temperatures in new samples of GdAg and DyAg were taken in order to confirm the results previously obtained. The anomalous behavior of the temperature dependence of mhf was analyzed with the proposed model to obtain the host contribution and the probe contribution to mhf. The probe contribution determined by the model was shown to agree with the expected experimental values. Host contribution obtained from the model were shown to follow the expected behavior for indirect magnetic coupling of rare-earth compounds and agree with the systematic behavior obtained from first-principles calculations using the density function theory (DFT), whose results also help to explain the mechanism responsible for the anomalous behavior of the temperature dependence of mhf.

2. Experimental

Samples of REAg were prepared by repeatedly melting the constituent elements (RE 99.99% and Ag 99.9985%) under argon atmosphere purified with a hot titanium getterer in an arc furnace. The samples used for PAC measurements were prepared in a similar way but with radioactive ^{140}La (obtained by neutron irradiation of

lanthanum metal) substituting about 0.1% of RE atoms. All samples were annealed under an atmosphere of ultra pure Ar for 48 h at 700 °C. The structure of each sample was checked by X-ray diffraction (XRD) measurements using Cu K_α with subsequent analysis by Rietveld method. The results indicated the cubic CsCl-type structure with the $Pm\bar{3}m$ space group for all samples and, within the resolution of XRD, no secondary phases were observed. Magnetization measurements were carried out for all samples in the temperature range of 4–200 K using a superconductor quantum interference device (SQUID), and the results are shown in Fig. 1.

The PAC measurements were carried out with a conventional fast-slow coincidence set-up with four conical BaF_2 detectors. The gamma cascade of 329 keV–487 keV, populated from the decay of ^{140}La, with an intermediate level with spin $I = 4^+$ at 2083 keV ($T_{1/2} = 3.45$ ns) in ^{140}Ce was used to measure the magnetic hyperfine field at the rare-earth sites. The samples were measured in the temperature range of 10–295 K by using a closed-cycle helium cryogenic device. The time resolution of the system was about 0.6 ns for the ^{140}Ce gamma cascade.

The PAC method is based on the observation of hyperfine interaction of nuclear moments with extra-nuclear magnetic field or electric field gradient. A detailed description of the experimental method can be found elsewhere [16,17]. The perturbation factor $G_{22}(t)$ of the correlation function, which contains detailed information about the hyperfine interaction, for an unpolarized ferromagnetic sample consisting of randomly oriented domains can be written (neglecting the A_{44} terms) as:

$$R(t) = A_{22}G_{22}(t) = A_{22}[0.2 + 0.4\cos(\omega_L t) + 0.4\cos 2(\omega_L t)] \quad (1)$$

Measurement of $G_{22}(t)$ allows the determination of the Larmor frequency $\omega_L = \mu_N g B_{hf}/\hbar$, from the known g-factor of the 2083 keV state of ^{140}Ce, and consequent determination of the magnetic hyperfine field B_{hf}. The experimental data for temperatures below T_N were analysed for a pure magnetic dipole interaction. This is because for ^{140}Ce the small value of the quadrupole moment ($Q = 0.35$ b [18]) and the short half-life (which delimit the time window for the observation of hyperfine interactions) of the intermediate state involved in the gamma cascade imply that only quadrupole interactions with frequencies much higher than those usually found in most materials could be observed. As a consequence, only magnetic dipole interactions might be observed with ^{140}Ce probe nuclei.

3. Results

The lattice parameter (a) of each compound was determined from XRD measurements and are displayed in Table 1, the results

Table 1
Weiss temperature, Néel temperature, and lattice parameter of REAg compounds.

Compound	θ (K)	T_N (K)	a (Å)
GdAg	−88.5	133	3.646
TbAg	−12.2	105	3.620
DyAg	−23.3	57	3.608
HoAg	−2.3	33	3.601

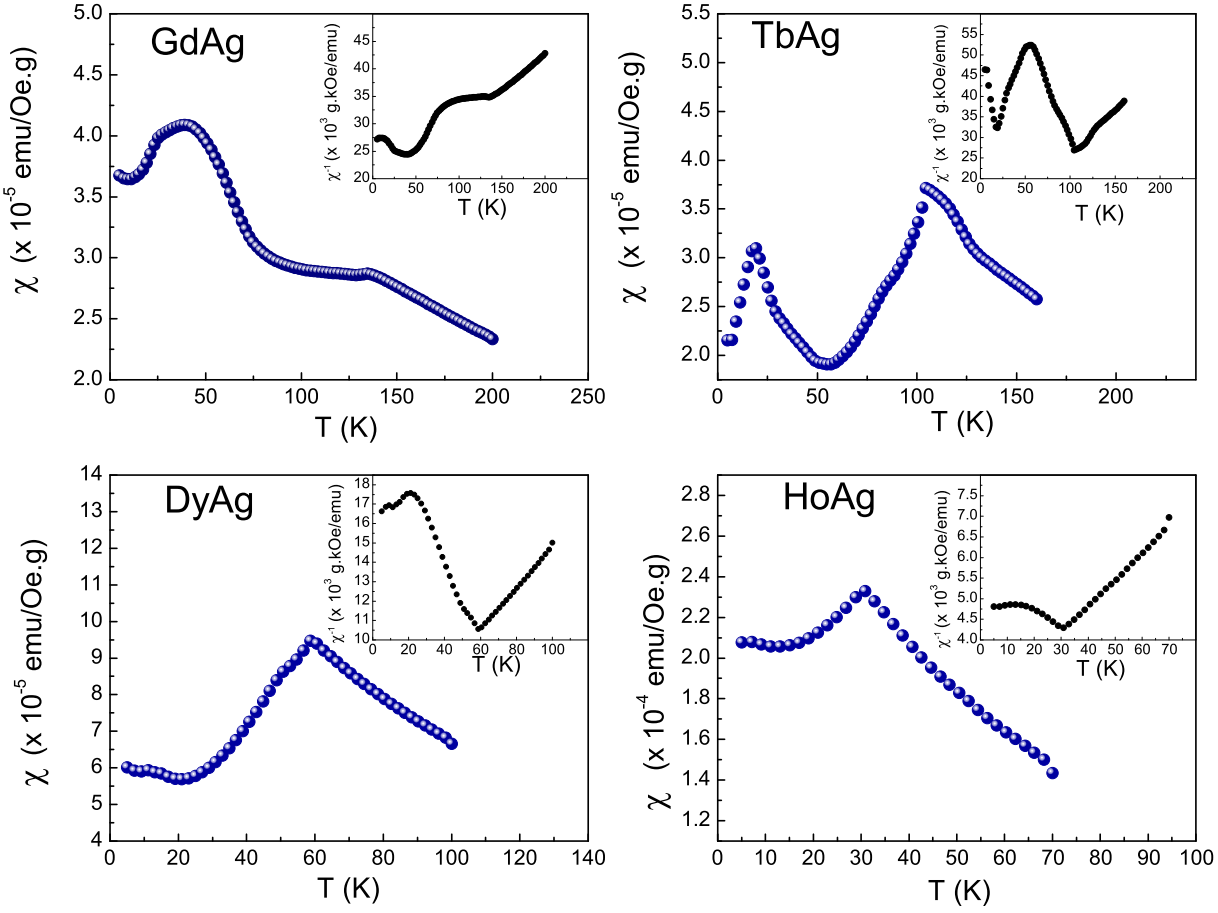

Fig. 1. Magnetic susceptibility χ(T) for REAg compounds in a magnetic field of 100 Oe. The insets show the inverse magnetic susceptibility χ^{-1}(T).

agree very well with those early reported [19]. Results from magnetization measurements show that the REAg compounds investigated in this work do not exhibit simple magnetic behavior, especially GdAg and TbAg. Therefore, the magnetization data from Fig. 1 for all compounds were fitted with the Curie–Weiss law $\chi(T) = \chi_0 + C/(T - \theta)$. The Weiss temperature (θ) obtained from the fit to the susceptibility data along with the Néel temperature (T_N) obtained from magnetization data are also presented in Table 1. Results are quite similar to those reported by Walline and Wallace [12].

Typical PAC spectra at some temperatures for GdAg and TbAg, measured by using the ^{140}La → ^{140}Ce probe, obtained just above and below respective Néel temperatures are shown in Fig. 2. Solid curves represent the least squares fit of the experimental data to Eq. (1). Results of the fitting indicated that most of the alloys had unique field with small distribution.

The PAC results show well-defined magnetic dipole interaction below the respective magnetic transition temperatures for both compounds. Fig. 3 shows the temperature dependence of the hyperfine field B_{hf} at ^{140}Ce in REAg compounds. The observed magnetic interaction corresponds to the antiferromagnetic ordering of the RE moments. However, mhf data show an accentuated deviation from the expected behavior for a simple antiferromagnetic ordering.

4. Discussion

The unusual behavior of B_{hf} with temperature (see Fig. 3) can be

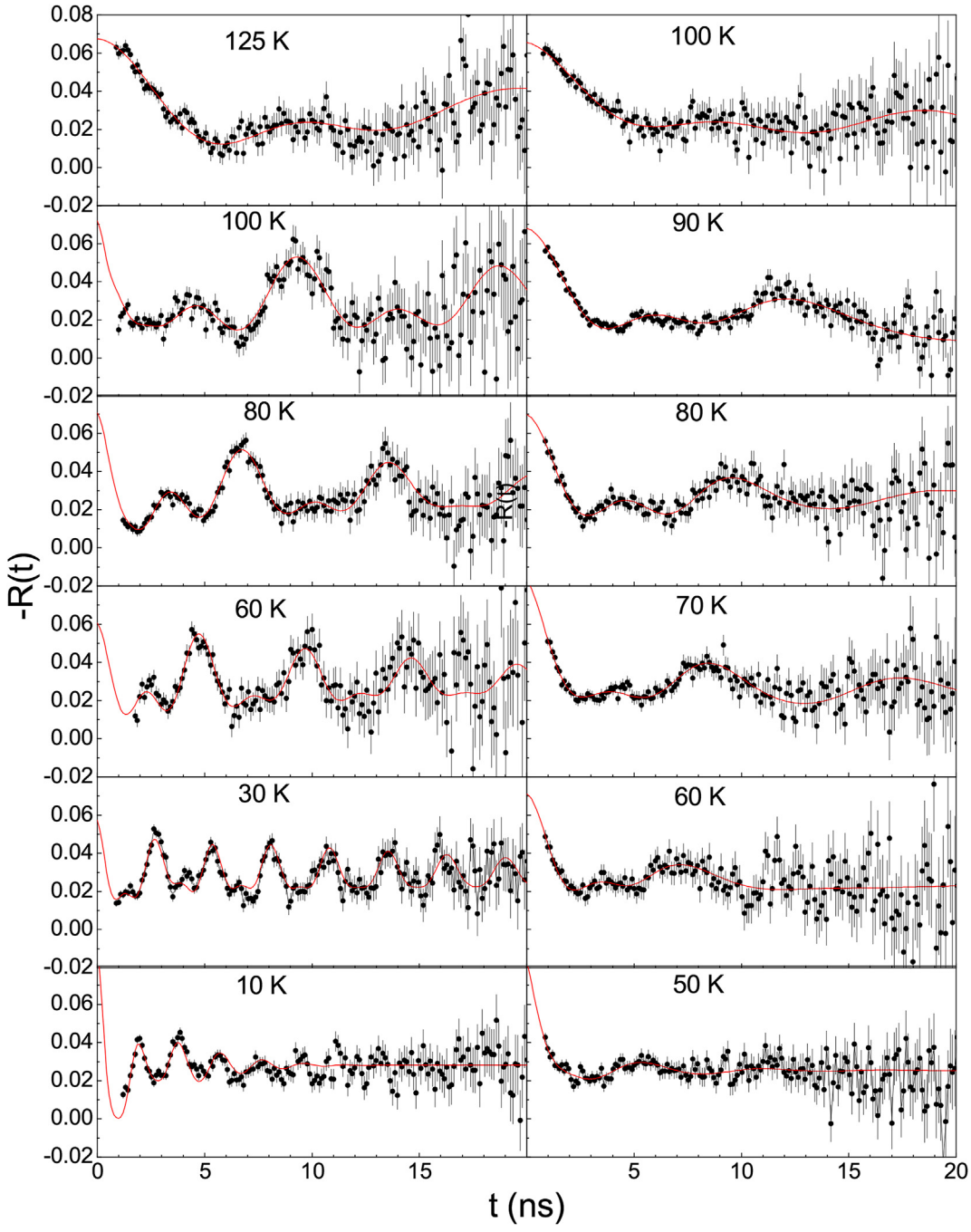

Fig. 2. Perturbation functions $R(t)$ of the ^{140}Ce probe in GdAg (left) and TbAg (right) at some temperatures below their respective Néel temperatures.

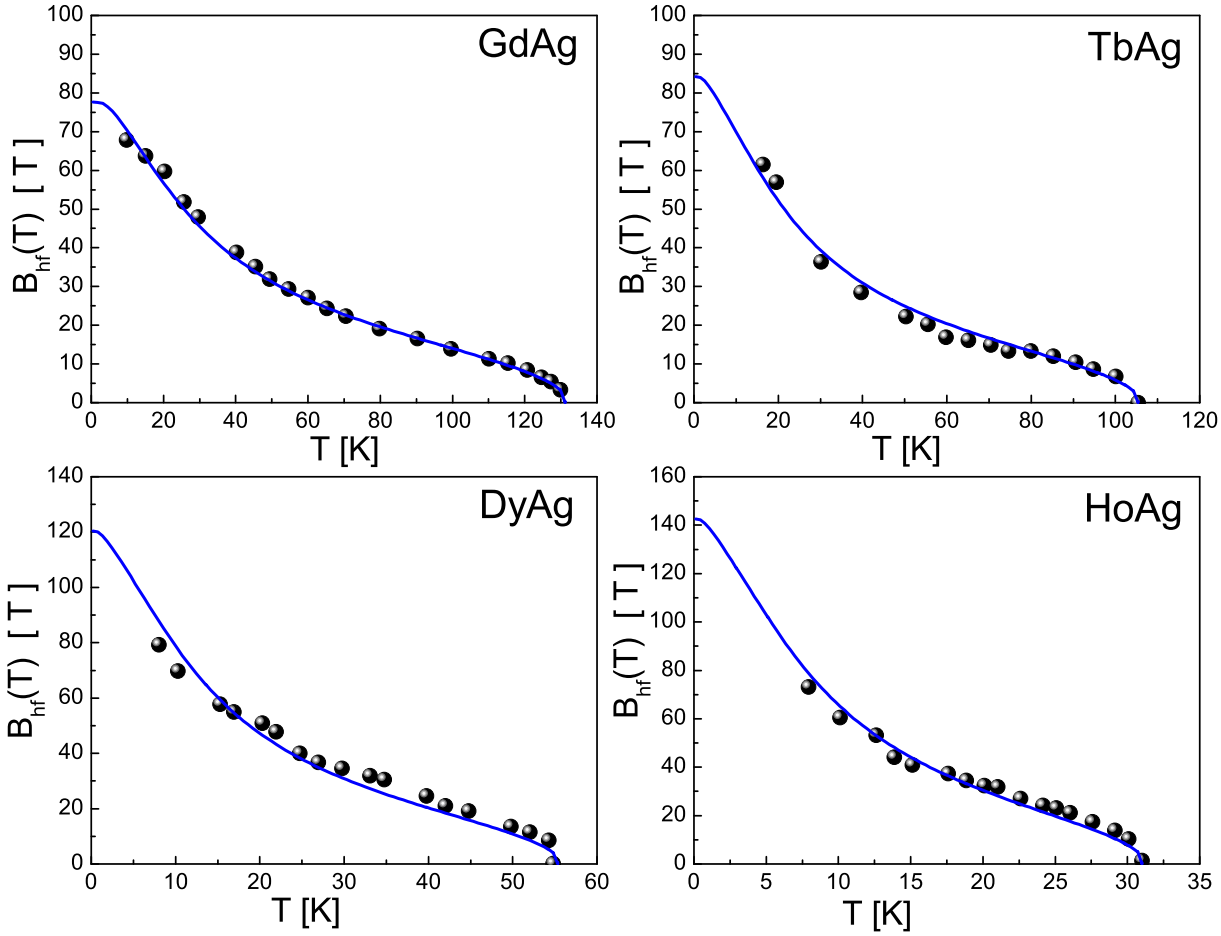

Fig. 3. Temperature dependence of the magnetic hyperfine field at RE sites in REAg measured with ^{140}Ce probe. The solid lines represent the fitting to a molecular field model described in the text.

explained by using a model derived from that used by Jaccarino et al. [20] to explain a similar behavior for the temperature dependence of the ^{55}Mn NMR frequency in ferromagnetic FeMn alloys. In order to explain such behavior the authors proposed a calculation of the NMR frequency based on a molecular-field theory in which the localized moment on Mn is oriented in the exchange field of Fe host. This model was modified by Bernas and Gabriel [21] in order to explain the temperature behavior of the mhf measured with a rare-earth probe nucleus ^{169}Tm in iron host and afterwards used to analyze results from PAC measurements using ^{140}Ce diluted in magnetic rare-earth hosts [2,22]. In this paper, a modification of the models used by those authors has been introduced. The effective hyperfine field, B_{hf}, at the probe site is given by the sum of the contributions from the probe ion itself, B^i_{hf} and from the polarization of conduction electrons by the magnetic ions of the host, B^h_{hf}, which scales with the host reduced magnetization $\sigma(T)$. B^i_{hf} is proportional to the thermal average of the impurity moment $\langle J^i \rangle$, which is localized and has magnitude independent of temperature. The thermal average of the localized magnetic moment of the impurity is taken over its levels in the exchange field of the host B^i_{exc}[20]:

$$B_{hf}(T) = B^i_{hf}(0) \times B_{J^i}(y) + B^h_{hf}(0)\sigma(T), \tag{2}$$

where the argument of the Brillouin function $B_{J^i}(y)$ is given by

$$y = \frac{\mu_B\left(g_{J^i} - 1\right)}{kT}\vec{J^i} \cdot \vec{B_{exc}}(T), \tag{3}$$

where μ_B and k are the Bohr magneton and the Boltzmann constant, respectively, the Landé factor $g_{J^i} = 6/7$ and total angular momentum $J^i = 5/2$ for Ce^{3+}. T is the temperature in all equations. The exchange field, which also scales with $\sigma(T)$, is given by

$$B_{exc}(T) = B_{exc}(0)\xi\sigma(T), \tag{4}$$

where ξ is a parameter that takes into account the fact that the host-impurity exchange may be different form the host–host exchange, and

$$B_{exc}(0) = \frac{3kT_o}{\left(g_{J^h} - 1\right)\left(J^h + 1\right)\mu_B}, \tag{5}$$

where T_o is the magnetic ordering transition temperature and, g_{J^h} and J^h are respectively the Landè factor and total angular momentum of the magnetic ion of the host. As REAg compounds studied in this work order antiferromagnetically, T_o is the Néel temperature, T_N. The temperature dependence of the B_{hf} for studied REAg compounds is shown in Fig. 3, where the solid curve represents the Eq. (2) described in this model, which better fit to the experimental data. In Table 2 the results for the relevant

Table 2
Parameters obtained from the fit of the model described in the text for the studied compounds.

Compound	J^h	g_{J^h}	T_N (K)	$B^i_{hf}(0)$ (T)	$B^h_{hf}(0)$ (T)	ξ
GdAg	7/2	2	132	−70	7.5	0.148
TbAg	6	3/2	106	−78	6.2	0.143
DyAg	15/2	4/3	56	−115	5.4	0.157
HoAg	8	5/4	31.5	−138	4.5	0.175

parameters obtained by fitting this model to the experimental data are also shown. The ξ values presented in the table were normalized to $\frac{(g_{J^h}-1)J^h}{(g_{Ji}-1)Jr}$.

We also have investigated the critical behavior near the transition temperature of each sample by least-square fitting only B_{hf} values immediately below T_N in Fig. 3 to the function $B(T) = B(0)(1 - T/T_N)^{\beta}$. The results of the fit are shown in Table 3 and the resulting transition temperatures T_N are in very good agreement with those obtained by magnetization measurements and those reported in literature shown in Table 1. The values for β are near to the theoretical value expected for a three dimensional isotropic Heisenberg magnet ($\beta \approx 0.38$).

4.1. First-principles calculations

In order to have a clear view of the electronic structure in the REAg plus Ce impurity, self-consistent calculations from the density functional theory [23] have been performed using the WIEN2k computer code [24], in which the Kohn-Sham equation in the crystal is solved by the augmented plane wave plus local orbitals(APW + lo) all-electron method. The muffin-tin sphere radius $R_{MT} = 2.9$ was chosen for the rare-earth and Ag. The number of plane-waves was limited by the cut-off $K_{max} = 7/R^{min}_{MT}$, and the charge density was Fourier expanded up to $G_{max} = 14$. For the Brillouin zone integration of the supercell, a mesh of 1600 k points was used within the whole zone. Exchange and correlation effects were treated with local density approximation (LDA) [23] which is parameterizated by Perdew-Wang [25]. The valence states were treated within the scalar-relativistic approach taking into account the spin–orbit interaction and the core states are relaxed in a fully relativistic manner. A supercell was used to simulate the antiferromagnetism and cerium dilution in each REAg-Ce system. These supercells were built up from $2\sqrt{2} \times 2\sqrt{2} \times 2$ REAg single-cell with a total of 32 atoms (16 of each element), in which one atom of host RE with majority spin was replaced by one Ce atom producing a concentration of 6.25% of Ce doping. An additional set of calculations was performed taking into account the local correlation from RE 4*f* electrons as treated directly by Hubbard parameter *U* into an approximation [26] for self interaction correction (DFT + *U*; the *U* value for all RE atoms is 6.8 eV, except for Gd, which has semi-filled 4*f* shell. In all calculations the charge difference between two self-consistent cycles was used as a convergence criterion.

Table 3
Parameters obtained from the fit of the function $B(T) = B(0)(1 - T/T_N)^{\beta}$ to data in the critical region.

compound	$B(0)$ (T)	β	T_N (K)
GdAg	25 (1)	0.41 (3)	131 (1)
TbAg	23 (1)	0.41 (5)	105 (1)
DyAg	48 (5)	0.35 (9)	54 (2)
HoAg	42 (5)	0.4 (1)	31 (3)

Results of calculations for mhf, determined by the methodology implemented in the WIEN2k code by Blugel [27], at Ce replacing RE sites in REAg structure are displayed in Table 4. It is well-known that the mhf calculated by *ab initio* methods based on DFT does not agree very well with the experimental values [28,29]. However, more important than the absolute values, we are interested in the behavior of these values as a function of determined parameters related to the magnetic coupling as will be discussed in the next subsections.

The partial *f* and *d* density of states projected on Ce, Gd and Ag extracted from calculations for Ce-doped GdAg supercell is displayed in Fig. 4. We have chosen to exhibit the Gadolinium atom with spin-up states (DOS from Gd with spin-down states has reciprocally majority states exchanged by the minority ones). Although the figure displays the GdAg compound it is representative of the PDOS for all REAg studied in this paper because, increasing the number of 4*f* electrons, the only difference in the PDOS plots will be the gradual population of the spin down RE 4*f* band (minority spin), with the Fermi level moving towards the conduction band. One can observe that the *d* bands are very wide, extending from −5.5 eV to ~2 eV, with the higher population region in the range from −5.5 eV to −4.0 eV, corresponding to the Ag 4*d* band fully filled. The inset in Fig. 4 shows that, for energies higher than −4 eV, all *d* bands are strongly hybridized with a very small population below the Fermi level, as expected. The figure also shows that the Gd spin-up 4*f* band is well-defined and far from the Fermi level, whereas the spin-down 4*f* band is unpopulated. Ag ion shows a full *d* band far from the Fermi level and, although it does not directly contribute to the magnetic interactions, Ag ions plays an important role in REAg compounds. Ag ions keep RE ions apart from each other making a direct *d*–*d* interaction between them less probable [33,34]. Moreover, the Ag ions are also important to provide *s* electrons to the conduction band helping in the indirect RKKY coupling via polarization of the conduction electrons. The DFT calculations corroborate the conclusion extracted from the systematic of $B^h_{hf}(0)$, which is described in the next subsection, that the indirect RKKY is the mechanism of coupling between the RE magnetic ions in REAg.

4.2. Host contribution to B_{hf}

The application of the model used to fit the temperature dependence of B_{hf} results in two contributions for the B_{hf}. One contribution comes from the polarization of the magnetic moment of the probe ion, B^i_{hf}. The other, $B^h_{hf}(0)$ comes from the magnetic rare-earth ions. This later contribution is due to unpaired localized 4*f* electrons in rare-earth ions. As 4*f* electrons are well localized, the magnetic coupling between these electrons of two nearest neighbor rare-earth ions occurs, therefore, by indirect exchange. There are two models which explain such exchange. The first model comes from the works of Ruderman and Kittel [30], Kasuya [31], and Yosida [32] and is known as RKKY theory in which exchange interactions between magnetic ions in metals is mediated by conduction electrons. The localized 4*f* electrons in the rare-earth ions

Table 4
Magnetic hyperfine field at Ce impurity calculated by WIEN2k code: core field (B_{core}) calculated from 1s, 2s, 3s, and 4s shells, valence field ($B_{valence}$) calculated from 5s to 6s shells of Ce, and the contact field ($B_{contact}$). All values are in Tesla.

compound	$B_{valence}$	B_{core}	$B_{contact}$
GdAg	25.48	−21.34	4.14
TbAg	21.46	−18.48	2.98
DyAg	21.38	−19.04	2.34
HoAg	19.36	−18.38	0.98

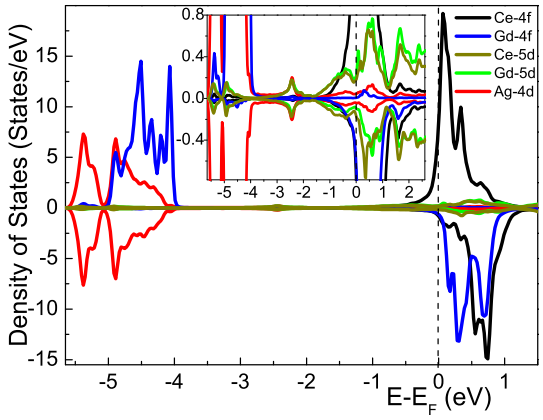

Fig. 4. Partial *d* and *f* density of states projected on Ce, Gd, and Ag for the studied REAg compounds. The inset displays the *d* contribution from Gd and Ce and shows that they are quite similar, however, very small and wide. It also shows that the *d* band of Ag is narrower with a high population. The dotted line indicates the position of the Fermi energy.

spin-polarize the conduction electrons, which in turn couples to the neighbor localized 4*f* electrons. In the second model, the indirect 4*f*–4*f* exchange is mediated by an intra-atomic 4*f*–5*d* polarization followed by a 5*d*–5*d*-exchange interaction between the spin polarized 5*d*-electrons of neighboring rare-earth ions [33,34]. In both cases, a spin polarization arises, which leads, via Fermi contact interaction, to a magnetic hyperfine field B_{hf} at the nucleus of a probe atom. In the RKKY interaction, polarized conduction *s*-character electrons induce a non-zero spin density at the probe nuclei, whereas in the 4*f*–5*d* interaction, 5*d* electrons of ^{140}Ce probes are directly polarized by the 5*d* electrons of the rare-earth host producing the magnetic hyperfine field.

Since spin exchange is the dominant mechanism in the polarization, the hyperfine magnetic field is expected to be proportional to $(g_{J^h}-1)J^h$, the spin projection of S along J^h. Therefore, in most rare-earth ferromagnets one finds that the relation B_{hf} vs. $(g_{J^h}-1)J^h$ is in fact approximately linear [35]. To verify this linearity, we have plotted in Fig. 5 values of $B^h_{hf}(0)$, from Table 2, as a function of $(g_{J^h}-1)J^h$ for each REAg compound. A linear function (solid straight line in the figure) fits very well the data and constitutes a strong indication that spin polarization by RKKY mechanism is responsible by the hyperfine fields at ^{140}Ce probes and also that the model used to fit the temperature dependence of B_{hf} can provide values for the host contribution (B^h_{hf}) which follows an expected behavior. Values of $B_{contact}$ displayed in Table 4 from DFT calculations are also shown in Fig. 5. As it was mentioned above, the values of B_{hf} calculated by DFT are often underestimated and do not agree with the experimental values. However, here we are interested in the systematic behavior of $B_{contact}$. As can be seen in the figure, $B_{contact}$ values show a linear dependence on $(g_{J^h}-1)J^h$ and were also fitted by a straight line with a slope (2.02 ± 0.19) very similar to that (1.96 ± 0.15) used to fit $B^h_{hf}(0)$. The straight line that fits $B_{contact}$ is displaced from that for B^h_{hf} because the constant terms extracted from the linear fits to each set of values are quite different: -2.95 ± 0.53 and 0.51 ± 0.43, respectively. This difference (~3.4 T) reflects the inaccuracy of the DFT calculations to reproduce the mhf values. Results from calculations, therefore, confirm the observed linear dependence on the spin projection of the B^h_{hf} and reinforce the conclusion that the model can provide values that follow an expected behavior.

The DFT + *U* calculations did not yield results as good as those for calculations without *U*. First, because the resulting $B_{contact}$ values do not follow the expected behavior as those determined from experimental data through Eq. (2) and displayed in Fig. 5. Second, the 4*f* peak for Ce impurity in the PDOS obtained from DFT + *U* calculations is located around 2 eV below the Fermi level, which is not expected. And last, the DFT + *U* calculations is not completely variational.

Since the relative values are shown to follow an expected behavior, we can now verify if the absolute values of $B^h_{hf}(0)$ obtained from the fit of the model to experimental data are reasonable. We have compared the result for GdAg with results of B_{hf} also measured with ^{140}Ce for other Gd compounds (GdNiIn [36,37], $GdNi_2$ [38] and $GdCo_2$ [39]) for which the behavior of the temperature dependence is reproduced by a Brillouin curve, which means that little, if any, 4*f* electron contribution is present and does not change the expected behavior of the host magnetization dominated by spin exchange mechanism. In the RKKY theory of indirect coupling, the magnetic ordering temperature (T_O) is expected to be proportional to the de Gennes factor [6,40]:

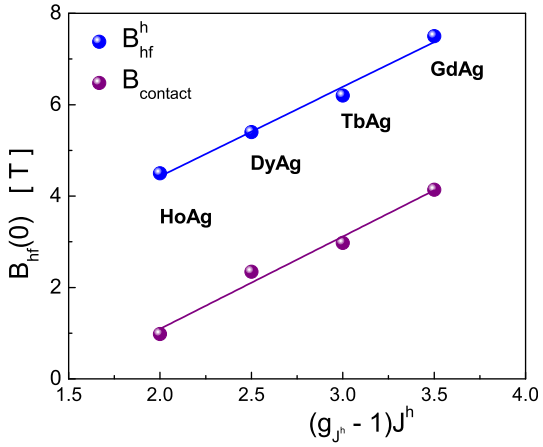

Fig. 5. Contribution from the RE ions of the host to the effective B_{hf} at T = 0 in REAg at ^{140}Ce as a function of the projected RE spin $(g_{J^h}-1)J^h$. Values were calculated with the model described in the text (B^h_{hf}) and simulated by first-principles calculations ($B_{contact}$). The solid lines represent the linear fit to the values.

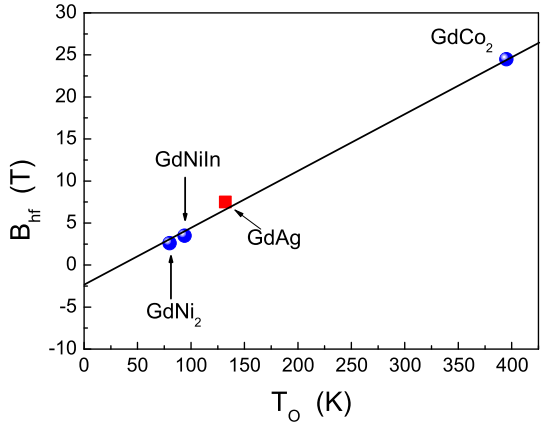

Fig. 6. Experimental values of B_{hf} extrapolated to T = 0 in some Gd compounds measured with ^{140}Ce probe as a function of respective magnetic ordering temperature. Data for GdAg, shown as a full red square, is that for the host contribution (B^h_{hf}) calculated by the model described in the text. The solid line represents the linear fit to B_{hf} values. (For interpretation of the references to colour in this figure legend, the reader is referred to the web version of this article.)

$T_O \propto \Gamma_{sf}^2 (g_{J^h} - 1)^2 J^h (J^h + 1)$, where Γ_{sf} is the *s-f* exchange constant. As $B_{hf}^h(0)$ has a linear dependence with $(g_{J^h} - 1)J^h$, the ratio B_{hf}^h/T_O is proportional to $[\Gamma_{sf}^2 (g_{J^h} - 1)(J^h + 1)]^{-1}$ and the plot of B_{hf}^h as a function of T_O must be, therefore, a straight line. Fig. 6 displays experimental values of B_{hf} at ^{140}Ce for GdNiIn, $GdNi_2$ and $GdCo_2$ compounds as a function of T_O. The value of $B_{hf}^h(0) = 7.5$ T for GdAg resulting from the fit of the model described by Eq. (2), follow the same linear relation between B_{hf} at ^{140}Ce and the magnetic transition temperature already observed for those compounds, as shown in Fig. 6. Therefore, the model used to fit the anomalous temperature dependence of B_{hf} measured with ^{140}Ce is able to provide values for the host contribution to the magnetic hyperfine field that are in very good agreement with those expected by the indirect coupling RKKY model.

4.3. Probe ion contribution to B_{hf}

The results of the fit also show that the values for $B_{hf}^i(0)$ are much higher than $B_{hf}^h(0)$ and have opposite signs for all compound. This contribution to the magnetic interaction is due to the polarization of *f*-spin moments of ^{140}Ce induced by the magnetic field from rare-earth moments [3]. As $B_{hf}^i(0)$ for all compounds is smaller than the magnetic hyperfine field of 183 T for the free Ce^{3+} ion [41], we suppose that the ground state for Ce ions is affected in a certain degree consequently resulting in an intermediate valence for Ce impurity ions.

In order to verify the quality of the B_{hf}^i values given by the model, we have compared them to the reduced magnetic hyperfine field B_{hf}/μ_{eff}, where μ_{eff} is the effective magnetic moment of the RE ion of the host compound. The magnetic hyperfine field at ^{140}Ce impurities on rare-earth sites can be considered as a sum of two main contributions:

$$B_{hf} = B_{hf}^i + B_{hf}^h. \tag{6}$$

The reduced B_{hf} can, thus, be written as

$$\frac{B_{hf}}{\mu_{eff}} = \frac{B_{hf}^i}{\mu_{eff}} + \frac{B_{hf}^h}{\mu_{eff}}. \tag{7}$$

The host contribution can be written as a sum of the partial contribution from the neighboring magnetic moment $\mu_{eff}(r_i)$ at the r_i position to the conduction electron polarization $p(r_i)$ [16]: $B_{hf}^h = A \sum \mu_{eff}(r_i) p(r_i)$, with A being the hyperfine coupling constant, which depends on the probe nucleus. As rare-earth atoms contribute with the same number of electrons to the conduction band and each compound has the same structure with almost the same lattice parameter, the last term in Eq. (7) will not appreciably vary for the REAg compounds. The main variation comes, therefore, from the first term. The reduced B_{hf}^i/μ_{eff} values calculated with B_{hf}^i (from Table 2) obtained from the fit of the model described above are shown in Fig. 7 as a function of the total RE angular momentum J^h. The results are compared with the experimental values of B_{hf}/μ_{eff}, also plotted in Fig. 7, where the values of B_{hf} where taken at temperatures $T = 0.24T_N$ for each compound in order to normalize them to that for HoAg, which has the lowest T_N among the studied compounds. This procedure is necessary to take into account the different T_N temperatures of the compounds that affects the saturation of B_{hf} at low temperatures.

The comparison of the experimental B_{hf}/μ_{eff} with the calculated B_{hf}^i/μ_{eff} shows a remarkable similar behavior with an increase of values when J^h increases from Gd to Ho. Values are different mainly because they were taken at different temperatures. However, if we consider, for instance, the value of $B_{hf} \sim 70$ T at the lowest measured temperature for GdAg, almost at the saturation region, $B_{hf}/\mu_{eff} \sim 8.1$ T/μ_B, which is practically equal to $B_{hf}^i/\mu_{eff} \sim 8.2$ T/μ_B calculated with the value obtained from the fit of the model shown in Table 2. The model used to fit the anomalous temperature dependence of B_{hf} measured with ^{140}Ce is also able to provide values for the ^{140}Ce impurity contribution to the magnetic hyperfine field which are in very good agreement with those expected from experiments.

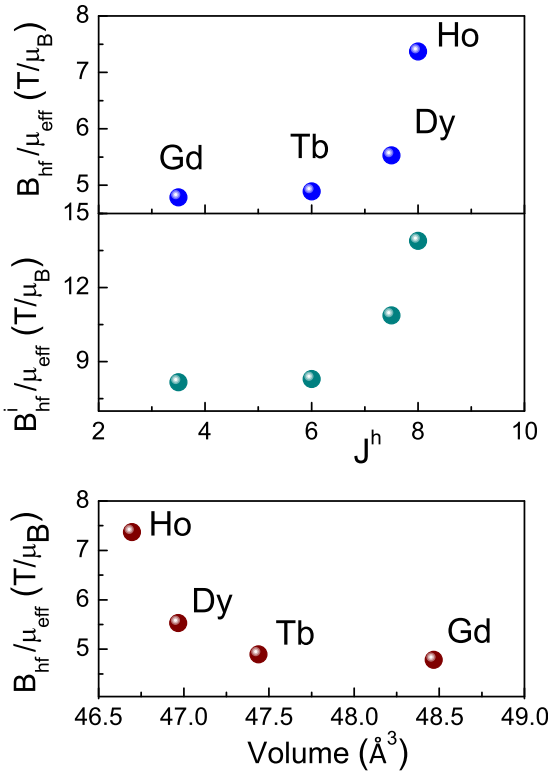

Fig. 7. Experimental reduced B_{hf}/μ_{eff} at temperatures equal to $0.24T_N$ (top) and calculated reduced B_{hf}^i/μ_{eff} at $T = 0$ K (middle) as a function of the total spin J^h of RE. The experimental B_{hf}/μ_{eff} as a function of the volume of unit cell for each REAg compound (bottom).

4.4. The anomalous behavior of B_{hf}: impurity-host magnetic interaction

The magnetic interaction between a magnetic impurity ion diluted in a magnetic host is still an issue not well understood. Some papers have studied the systematic of the magnetic hyperfine field at different impurities (magnetic and non-magnetic) on ferromagnetic hosts, especially in iron, with the only intention of explain the dependence of mhf on the atomic number of the impurity [42,43]. Nevertheless, the host-impurity exchange interaction, when both are magnetic, in particular, is not well described so far and few works attempted to understand this issue using different mathematical approach [44,45], however, without explanation about the physical origin of the anomalous behavior of the temperature dependence of B_{hf}. In the model described above the strength of the host-impurity interaction is approximated by the parameter ξ, the higher its value the weaker is the host-impurity exchange interaction. The results of the fitting (see Table 2) show that this parameter roughly increases with the increase of the rare-earth total spin J^h revealing that the host-

impurity interaction slightly weakens when going from Gd ($J = 7/2$) to Ho ($J = 8$).

The data of B_{hf} at ^{140}Ce in REAg are, therefore, also useful to investigate the, so far, not well understood issue, *i.e.* the behavior of localized magnetic moments at dilute magnetic impurities in a magnetic matrix. The clear observable evidence of such a phenomenon is the anomalous behavior of the temperature dependence of B_{hf} measured at probe nuclei of magnetic elements as diluted impurities in magnetic hosts. Shirley et al. reported a first review about mhf at transition metal impurities in magnetic transition metal hosts [46].

Recently, in an attempt to explain the origin of this phenomenon, the mhf at ^{140}Ce probes in $RERh_2Si_2$ (RE = Ce, Pr, Nd, Gd,Tb, Dy) compounds was measured as a function of temperature [47] and results indicated a strong correlation between the reduced B_{hf}, which is proportional to the probe contribution to mhf, and the unit cell volume. Using the prediction of the Anderson model, which states that the hybridization of the 4*f* band with conduction electrons is inversely proportional to the unit cell volume [48], the authors concluded that hybridization could play an important role in the ^{140}Ce impurity contribution [47]. The higher is the unit cell volume the lower is the hybridization and, consequently, the higher is the Ce 4*f* contribution to B_{hf}, i.e., the higher is the reduced B_{hf}. For $GdRh_2Si_2$, the only compound in the studied series that presented an anomalous temperature dependence of B_{hf} [49], this contribution is the lowest observed with a consequent stronger hybridization, which was assigned as the responsible for the anomalous behavior of the temperature dependence of B_{hf} [47]. In the work reported here, the reduced B_{hf} showed an opposite correlation with the cell volume (see Fig. 7), the higher is the unit cell volume the lower is the reduced B_{hf}. These results, therefore, imply that, differently from $GdRh_2Si_2$, hybridization does not play an important role in the anomalous temperature dependence of B_{hf} in REAg compounds and a different mechanism of reducing the Ce 4*f* occupation (and, consequently, the contribution to B_{hf}) with temperature must be acting.

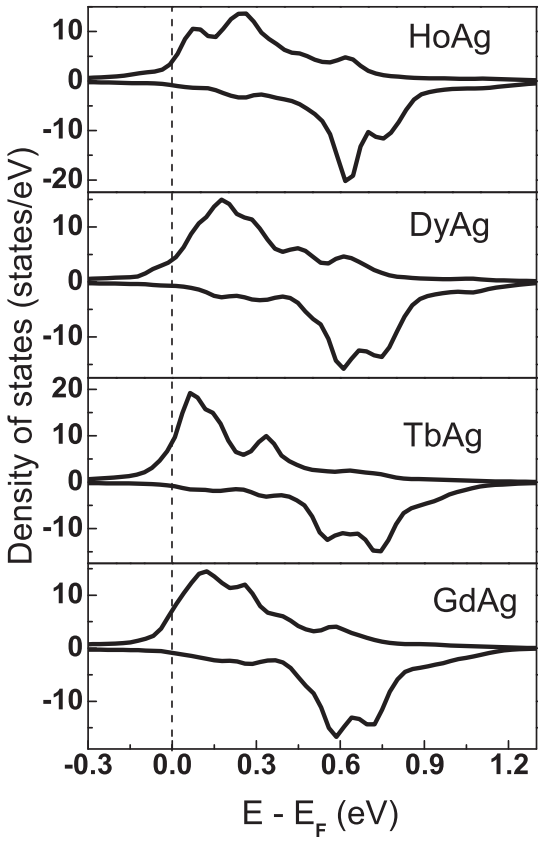

Fig. 8. 4*f* states from the total density of states projected on Ce for the studied REAg compounds. The dotted line indicates the position of the Fermi energy.

Total density of states projected on Ce for Ce-doped REAg (RE = Gd, Tb, Dy, Ho) compounds are shown in Fig. 8. It is clearly seen from the figure that the Ce 4*f* band defines the Fermi level and it is scarcely occupied (it is occupied by less than one electron). These results qualitatively agree with those obtained from the proposed model. The values of B^i_{hf} indicate that the 4*f* band would not be fully occupied.

Taking into account the first-principles calculations, we then propose that the position of the Ce 4*f* band is the key to explain the behavior of the temperature dependence of B_{hf} in REAg compounds measured with ^{140}Ce. Consequently, the decrease of B_{hf} with temperature experimentally observed is due to the gradual delocalization of the Ce 4*f* electron when the temperature increases. If the 4*f* band is at the Fermi level or very close to it at 0 K, when the temperature increases the band moves towards and beyond the Fermi level and the contribution of the 4*f* electrons from the Ce impurity atoms to the measured B_{hf} decreases. As a result, a strong decrease is observed, when compared to the Brillouin curve, in the temperature dependence of B_{hf}.

5. Conclusion

The use of ^{140}Ce as a nuclear probe for measurements of the magnetic hyperfine field via PAC spectroscopy in the rare-earth compounds REAg (RE = Gd, Tb, Dy, Ho) was investigated. For all studied compound, B_{hf} showed an anomalous dependence with temperature with a deep decrease when temperature increases. This behavior was ascribed to the contribution from the 4*f* electron of Ce impurity (B^i_{hf}) to the total B_{hf} in addition to the host contribution (B^h_{hf}) from the RE ion of the compound. A model based on the molecular field theory and capable to differentiate these two contributions was used to fit the temperature dependence of B_{hf} of all samples. The resulting B^h_{hf} values show a linear dependence on the RE spin projection $(g_{J^h} - 1)J^h$, indicating that these values obtained from the fit follow an expected behavior. Moreover, DFT calculations results for the contact field contribution also show the same systematic behavior, confirming, therefore, that B^h_{hf} calculated by the proposed model give values that really correspond to the host contribution. Furthermore, the comparison of the B^h_{hf} value for GdAg with experimental B_{hf} values, also measured with ^{140}Ce, for other Gd compounds, for which the temperature dependence follows the expected Brillouin curve, has shown that the calculated value of B^h_{hf} from the fit follows the same linear dependence with the magnetic ordering temperature indicating that the fit produced a B^h_{hf} value with an intensity that agrees very well with an experimental systematical behavior. As for the Ce impurity contribution B^i_{hf} obtained by the fit, it was possible to compare it with the experimental values B_{hf}/μ_{eff} and verify that both follow the same systematics with intensities very close each other. However, it was also verified that B_{hf}/μ_{eff} values decrease with the unit cell volume, conversely as observed in $RERh_2Si_2$ compounds [47]. This ruled out the supposition that hybridization of Ce 4*f* with host *d* electrons would play an important role in determining the anomalous behavior of the temperature dependence of B_{hf} in REAg. Therefore, we have proposed a different mechanism of such striking phenomenon in REAg, based on first-principles calculation: the position of the Ce 4*f* band relative to the Fermi level would have the chief role in determining the shape of the temperature dependence

of B_{hf}. In conclusion, the delocalization of the Ce 4*f* band is responsible by the decrease of B_{hf} with the temperature experimentally observed at ^{140}Ce probe nuclei dilute in a magnetic host. However, this delocalization can occur by different mechanisms, in $GdRh_2Si_2$ it was shown that the delocalization occurs indirectly by hybridization of Ce 4*f* band. In REAg compounds the delocalization occurs directly because the Ce 4*f* band is located at the Fermi level. The model presented in this paper does not explore details about the nature of ground state of the Ce impurity neither if the increase of temperature promotes the occupation of other states. This issue may be further investigated in order to obtain a more detailed description of the intriguing phenomenon here observed.

Acknowledgments

Partial support for this research was provided by the Fundação de Amparo á Pesquisa do Estado de São Paulo (FAPESP) (grant no. 2012/11104-9). AWC, JMF, LFDP and RNS thankfully acknowledge the support provided by the Conselho Nacional de Desenvolvimento Científico e Tecnológico (CNPq) in the form of research fellowships.

References

[1] L. Büermann, H.J. Barth, K.H. Biedermann, M. Luszik-Bhadra, D. Riegel, Observation of magnetic instabilities in dilute Pr, Nd, and Pm systems, Phys. Rev. Lett. 56 (1986) 492. http://dx.doi.org/10.1103/PhysRevLett.56.492.
[2] T.A. Thiel, E. Gerdau, B. Scharnberg, M. Böttcher, Time dependent hyperfine fields in intermediate valent ^{140}CeTb, Hyperf. Interact. 14 (1983) 347. http://dx.doi.org/10.1007/BF02043306.
[3] A.W. Carbonari, J. Mestnik-Filho, R.N. Saxena, M.V. Lalic, Magnetic hyperfine interaction in $CeMn_2Ge_2$ and $CeMn_2Si_2$ measured by perturbed angular correlation spectroscopy, Phys. Rev. B 69 (2004) 144425. http://dx.doi.org/10.1103/PhysRevB.69.144425.
[4] M. Forker, A. Hammesfahr, The magnetic hyperfine field at Cd nuclei in the rare earth ferromagnets Gd, Tb, Dy, Ho, Er and Tm, Z. Phys. 33 (1973). http://dx.doi.org/10.1007/BF02351860.
[5] P. de La Presa, S. Müller, A.F. Pasquevich, M. Forker, Investigation of the magnetic hyperfine field of ^{111}Cd in the rare-earth Laves phases RCo_2 and RNi_2, J. Phys. Condens. Matter. 12 (2000) 3423. http://dx.doi.org/10.1088/0953-8984/12/14/317.
[6] M. Forker, R. Müsseler, S.C. Bedi, M. Olzon-Dionysio, S.D. de Souza, Magnetic and electric hyperfine interactions in the rare-earth indium compounds R_2 in studied by ^{111}Cd perturbed angular correlations, Phys. Rev. B 71 (2005) 094404. http://dx.doi.org/10.1103/PhysRevB.71.094404.
[7] P. de La Presa, M. Forker, J. Th Cavalcante, A.P. Ayala, Spin and temperature dependence of the magnetic hyperfine field of ^{111}Cd in the rare earth-aluminum Laves phase compounds RAl_2, J. Magn. Magn. Mater. 306 (2006) 292. http://dx.doi.org/10.1016/j.jmmm.2006.03.029.
[8] K.H.J. Buschow, J.P. de Jong, H.W. Zandbergen, B. van Laar, Magnetic properties of some light rare?earth compounds with CsCl structure, J. Appl. Phys. 46 (1975) 1352. http://dx.doi.org/10.1063/1.321704.
[9] T. Chattopadhyay, G.J. McIntyre, U. Köbler, Antiferromagnetic phase transition in GdAg, Solid State Comm. 100 (1996) 117. http://dx.doi.org/10.1016/0038-1098(96)00358-4.
[10] J.W. Cable, W.C. Koehler, E.O. Wollan, Magnetic order in rare-earth intermetallic compounds, Phys. Rev. 136 (1964) A240. http://dx.doi.org/10.1103/PhysRev.136.A240.
[11] G. Arnold, N. Nereson, C. Olsen, Magnetic structure of DyAg, J. Chem. Phys. 46 (1967) 4041. http://dx.doi.org/10.1063/1.1840484.
[12] R.E. Walline, W.E. Wallace, Magnetic characteristics of lanthanide? silver compounds having the CsCl structure, J. Chem. Phys. 41 (1964) 3285. http://dx.doi.org/10.1063/1.1725726.
[13] F.H.M. Cavalcante, L.F.D. Pereira, A.W. Carbonari, J. Mestnik-Filho, R.N. Saxena, Magnetic hyperfine field at Nd sites in NdAg studied by perturbed angular correlation spectroscopy and ab-initio calculations, J. Magn. Magn. Mater. 322 (2010) 1130. http://dx.doi.org/10.1016/j.jmmm.2009.07.060.
[14] F.H.M. Cavalcante, A.W. Carbonari, J. Mestnik-Filho, R.N. Saxena, Temperature dependence of the magnetic hyperfine field at ^{140} Ce on Gd sites in GdAg compound, Hyperf. Interact. 158 (2004) 125. http://dx.doi.org/10.1007/s10751-005-9020-8.
[15] A.W. Carbonari, F.H.M. Cavalcante, L.F.D. Pereira, G.A. Cabrera-Pasca, J. Mestnik-Filho, R.N. Saxena, Magnetic field at ^{140} Ce in Dy sites in DyX (X=Cu,Ag) compounds studied by perturbed angular correlation spectroscopy, J. Magn. Magn. Mater 320 (2008) e478. http://dx.doi.org/10.1016/j.jmmm.2008.02.172.
[16] A.W. Carbonari, R.N. Saxena, W. Pendl Jr., J. Mestnik-Filho, R.N. Attili, M. Olzon-Dionysio, S.D. de Souza, Magnetic hyperfine field in the Heusler alloys Co_2YZ (Y = V, Nb, Ta, Cr; Z = Al, Ga), J. Magn. Magn. Mater. 163 (1996) 313. http://dx.doi.org/10.1016/S0304-8853(96)00338-1.
[17] R. Dogra, A.C. Junqueira, R.N. Saxena, A.W. Carbonari, J. Mestnik-Filho, M. Morales, Hyperfine interaction measurements in $LaCrO_3$ and $LaFeO_3$ perovskites using perturbed angular correlation spectroscopy, Phys. Rev. B 63 (2001) 224104. http://dx.doi.org/10.1103/PhysRevB.63.224104.
[18] B. Klemme, H. Miemczyk, Proc. Int. Conf. Nucl. Moments and Nucl. Structure, Tokyo 1972, J. Phys. Soc. Jpn. 34 (1973) 265–266.
[19] K.H.J. Buschow, Intermetallic compounds of rare earths and non-magnetic metals, Rep. Prog. Phys. 42 (1979) 1373. http://dx.doi.org/10.1088/0034-4885/42/8/003.
[20] V. Jaccarino, L.R. Walker, G.K. Wertheim, Localized moments of manganese impurities in ferromagnetic iron, Phys. Rev. Lett. 13 (1964) 752. http://dx.doi.org/10.1103/PhysRevLett.13.752.
[21] H. Bernas, H. Gabriel, Experimental and theoretical study of perturbed angular correlations for a rare-earth localized moment in iron, Phys. Rev. B 7 (1973) 468. http://dx.doi.org/10.1103/PhysRevB.7.468.
[22] E. Wäckelgard, E. Karlsson, B. Lindgren, A. Mayer, Z. Hrynkiewicz, Hyperfine fields at Ce in $GdAl_2$ and $DyAl_2$, Hyperf. Interact. 51 (1989) 853–859. http://dx.doi.org/10.1007/BF02407792.
[23] W. Kohn, L.J. Sham, Self-consistent equations including exchange and correlation effects, Phys. Rev. 140 (1965) A1133. http://dx.doi.org/10.1103/PhysRev.140.A1133.
[24] P. Blaha, K. Schwarz, G.K.H. Madsen, D. Kvasnicka, J. Luitz, WIEN2k, an Augmented Plane Wave + Local Orbitals Program for Calculating Crystal Properties, Karlheinz Schwarz, Techn. Universität Wien, Autria, 2001, ISBN 3-9501031-1-2.
[25] J.P. Perdew, Y. Wang, Accurate and simple analytic representation of the electron-gas correlation energy, Phys. Rev. B 45 (1992) 13244. http://dx.doi.org/10.1103/PhysRevB.45.13244.
[26] V.I. Anisimov, I.V. Solovyev, M.A. Korotin, M.T. Czyzyk, G.A. Sawatzky, Density-functional theory and NiO photoemission spectra, Phys. Rev. B 48 (1993) 16929. http://dx.doi.org/10.1103/PhysRevB.48.16929.
[27] S. Blugel, H. Akai, R. Zeller, P.H. Dederichs, Hyperfine fields of 3d and 4d impurities in nickel, Phys. Rev. B 35 (1987) 3271. http://dx.doi.org/10.1103/PhysRevB.35.3271.
[28] P. Novák, V. Chlan, Contact hyperfine field at Fe nuclei from density functional calculations, Phys. Rev. B 81 (2010) 174412. http://dx.doi.org/10.1103/PhysRevB.81.174412.
[29] H. Akai, T. Kotani, Theory of hyperfine fields of iron, Hyperf. Interact. 120–121 (1999) 3. http://dx.doi.org/10.1023/A:1017057408403.
[30] M.A. Ruderman, C. Kittel, Indirect exchange coupling of nuclear magnetic moments by conduction electrons, Phys. Rev. 96 (1954) 99. http://dx.doi.org/10.1103/PhysRev.96.99.
[31] T. Kasuya, A theory of metallic ferro- and antiferromagnetism on Zener's model, Progr. Thoeoret. Phys. 16 (1956) 45. http://dx.doi.org/10.1143/PTP.16.45.
[32] Y. Yosida, Magnetic properties of Cu-Mn alloys, Phys. Rev. 106 (1957) 893. http://dx.doi.org/10.1103/PhysRev.106.893.
[33] I.A. Campbell, Indirect exchange for rare earths in metals, J. Phys. F 2 (1972) L47. http://dx.doi.org/10.1088/0305-4608/2/3/004.
[34] M.S.S. Brooks, O. Eriksson, B. Johansson, 3d–5d band magnetism in rare earth transition metal intermetallics: $LuFe_2$, J. Phys. Condens. Matter. 1 (1989) 5861. http://dx.doi.org/10.1088/0953-8984/1/34/004.
[35] M. Müller, P. de La Presa, M. Forker, The magnetic hyperfine field of ^{111}Cd in the rare earth? Nickel laves phases RNi_2, Hyperf. Interact. 158 (2004) 163. http://dx.doi.org/10.1007/s10751-005-9031-5.
[36] A.L. Lapolli, R.N. Saxena, J. Mestnik-Filho, D.M.T. Leite, A.W. Carbonari, Local investigation of magnetism at R and In sites in RNiIn (R=Gd, Tb, Dy, Ho) compounds, J. Appl. Phys. 101 (2007) 09D510. http://dx.doi.org/10.1063/1.2709421.
[37] A.L. Lapolli, A.W. Carbonari, R.N. Saxena, J. Mestnik-Filho, Investigation of hyperfine interactions in GdNiIn compound, Hyperf. Interact. 158 (2004) 157. http://dx.doi.org/10.1007/s10751-005-9029-z.
[38] A. W. Carbonari, unpublised.
[39] J. Mestnik-Filho, A.W. Carbonari, H. Saitovitch, P.R.J. Silva, Investigation of the magnetic hyperfine field at ^{140} Ce on Gd sites in $GdCo_2$ compound, Hyperf. Interact. 158 (2004) 189. http://dx.doi.org/10.1007/s10751-005-9028-0.
[40] P.G. de Gennes, Indirect interactions between 4f shells in rare earth metals, J. Phys. Radium 23 (1962) 510. http://dx.doi.org/10.1051/jphysrad:01962002308-9051001.
[41] B. Bleaney, in: R.J. Elliot (Ed.), Magnetic Properties of Rare Earth Metals, 383, Plenum, New York, 1972.
[42] G.N. Rao, Table of hyperfine fields for impurities in Fe, Co, Ni, Gd and Cr, Hyperf. Interact. 26 (1985) 1119. http://dx.doi.org/10.1007/BF02354655.
[43] D. Torumba, V. Vanhoof, M. Rots, S. Cottenier, Hyperfine interactions at lanthanide impurities in Fe, Phys. Rev. B 74 (2006) 014409. http://dx.doi.org/10.1103/PhysRevB.74.014409.
[44] S.W. Lovesey, Distribution of magnetization in mixed magnetic systems: III. Magnetic impurity, Proc. Phys. Soc. 89 (1966) 893. http://dx.doi.org/10.1088/0370-1328/89/4/313.
[45] T. Wolfram, W. Hall, Thermal properties of spin-wave impurity states, Phys. Rev. 143 (1966) 284. http://dx.doi.org/10.1103/PhysRev.143.284.
[46] D.A. Shirley, S.S. Rosenblum, E. Matthias, Hyperfine fields at solutes in ferromagnets: cadmium and ruthenium in nickel, Phys. Rev. 170 (1968) 363. http://dx.doi.org/10.1103/PhysRev.170.363.

[47] G.A. Cabrera-Pasca, A.W. Carbonari, B. Bosch-Santos, J. Mestnik-Filho, R.N. Saxena, The effect of hybridization on local magnetic interactions at highly diluted Ce ions in tetragonal intermetallic compounds $RERh_2$ Si_2 (RE=Ce, Pr, Nd, Gd, Tb, Dy), J. Phys. Condens. Matter 24 (2012) 416002. http://dx.doi.org/10.1088/0953-8984/24/41/416002.
[48] P.W. Anderson, Localized magnetic states in metals, Phys. Rev. 124 (1961) 41. http://dx.doi.org/10.1103/PhysRev.124.41.
[49] G.A. Cabrera-Pasca, A.W. Carbonari, R.N. Saxena, B. Bosch-Santos, J.A.H. Coaquira, J.A. Filho, Magnetic hyperfine field at highly diluted Ce impurities in the antiferromagnetic compound $GdRh_2$ Si_2 studied by perturbed gamma?gamma angular correlation spectroscopy, J. Alloys Compd. 515 (2012) 44. http://dx.doi.org/10.1016/j.jallcom.2011.10.077.